



Article

In Situ Measurements of Cirrus Clouds on a Global Scale

Gary Lloyd ^{1,2,*}, Martin Gallagher ¹ , Thomas Choularton ¹, Martina Krämer ³ , Petzold Andreas ⁴ and Darrel Baumgardner ⁵

¹ Centre for Atmospheric Science, University of Manchester, Manchester M13 9PL, UK; martin.gallagher@manchester.ac.uk (M.G.); choularton@manchester.ac.uk (T.C.)

² National Centre for Atmospheric Science (NCAS), University of Manchester, Manchester M13 9PL, UK

³ Forschungszentrum Jülich, IEK-7 Stratosphere, 52428 Jülich, Germany; m.kraemer@fz-juelich.de

⁴ Forschungszentrum Jülich, IEK-8 Troposphere, 52428 Jülich, Germany; a.petzold@fz-juelich.de

⁵ Droplet Measurement Technologies, Boulder, CO 80301, USA; darrel.baumgardner@gmail.com

* Correspondence: gary.lloyd@manchester.ac.uk

Abstract: Observations of high-altitude cirrus clouds are reported from measurements made during the routine monitoring of cloud properties on commercial aircraft as part of the In-Service Aircraft for a Global Observing System. The increasing global scale of the measurements is revealed, with 7 years of in situ data producing a unique and rapidly growing dataset. We find that cloud fractions measured ≥ 10 km at aircraft cruise altitude are representative of seasonal trends associated with the mid-latitude jet stream in the Northern Hemisphere, and the relatively higher cloud fractions are found in tropical regions such as the Inter-Tropical Convergence Zone and South East Asia. Both stratospheric and tropospheric data were used to calculate the cloud fractions routinely experienced by commercial aircraft. Further work is needed for a direct comparison with previous studies that limit cloud fraction calculations to tropospheric data only. The characteristics of these clouds are discussed and the potential different formation mechanisms in different regions assessed.

Keywords: cirrus; clouds; aviation; microphysics; aircraft; in situ



Citation: Lloyd, G.; Gallagher, M.; Choularton, T.; Krämer, M.; Andreas, P.; Baumgardner, D. In Situ Measurements of Cirrus Clouds on a Global Scale. *Atmosphere* **2021**, *12*, 41. <https://doi.org/10.3390/atmos12010041>

Received: 9 November 2020

Accepted: 28 December 2020

Published: 30 December 2020

Publisher's Note: MDPI stays neutral with regard to jurisdictional claims in published maps and institutional affiliations.



Copyright: © 2020 by the authors. Licensee MDPI, Basel, Switzerland. This article is an open access article distributed under the terms and conditions of the Creative Commons Attribution (CC BY) license (<https://creativecommons.org/licenses/by/4.0/>).

1. Introduction

In-Service Aircraft for a Global Observing System (IAGOS) is a European Research Infrastructure that combines the scientific expertise of its member institutions with the infrastructure of civil aviation to make near continuous measurements of the atmosphere on a global scale. The history of measurements on commercial aircraft dates back to 1994 through the Measurement of Ozone and Water Vapour on Airbus Aircraft (MOZAIC) and from the 2008 Civil Aircraft for the Regular Investigation of the Atmosphere Based on an Instrument Container (CARIBIC). From this, IAGOS-CARIBIC and IAGOS-CORE were developed, with the former involving 10–12 flights per year to make extensive measurements of the atmosphere using state-of-the-art instruments and the latter providing multiple flights per day across the globe using an automated instrument package mounted on multiple aircraft. Further information about the structure of IAGOS and planned future development can be found in [1].

Routine measurements by commercial aircraft over the past 25 years have enabled research on a multitude of essential climate variables (ECVs) [2] on a time scale that is important in the context of global climate change. This has included temperature trends [3], greenhouse gases including CO₂, CH₄, CO and H₂O [4,5] climatologies of O₃, CO and H₂O in the Upper Troposphere Lower Stratosphere (UTLS) [6–8] and cloud properties measured in situ [9,10]. This paper describes the long-term in situ observations of cirrus cloud macro-physical properties, location and frequency for the time period 2011–2018.

Cirrus is a broad term to describe high altitude ice clouds that can have very different origins and properties. The majority of cirrus in tropical regions is the result of convective thunderstorm outflow (detained cloud). In the mid latitudes, it is most often associated

with storm tracks driven by the sub-polar Jetstream, although cirrus from thunderstorm outflow can also be seen over mid-latitude continents during the summer months. Contrails formed by the hot moist exhaust products from jet engines can spread into cirrus and are among the most visible anthropogenic influences on the global radiation budget [11] and the only man-made ice clouds [12]. The global mean cover produced by these man-made line shaped contrails has been reported to be about 0.1% [13], resulting in a global and annual mean radiative forcing of 0.02 W m^{-2} [14]. This estimation is subject to large uncertainties with Fahey and Schumann reporting a likely range between 0.005 and 0.06 W m^{-2} for present day forcing [15].

Cirrus clouds cover large parts of the globe. In mid-latitudes, these high ice clouds cover 30% at any given time and in the tropics this can be 60–80% [16]. The radiative impact of cirrus clouds is one of the largest sources of uncertainty in global climate models (GCMs) due to the complex microphysical processes that are poorly understood and difficult to measure. The magnitude and even sign of the net radiative effect is very sensitive to these complexities that include properties such as the ice crystal size distribution, the ice crystal shape and the horizontal and vertical extent of the cloud [17]. Estimations of the radiative effect of these clouds is further complicated when considering the anthropogenic impact on their properties in the future, due to changes in the chemical and physical properties of aerosol particles and atmospheric dynamics as a result of a changing climate. Kärcher suggested that the microphysical and macrophysical representation of cirrus in GCMs must be advanced before we can accurately predict their impact on the global climate [18].

A major source of the uncertainty surrounding cirrus clouds is the challenging nature of measurements on the relevant scale that captures the evolution and dissipation of these clouds [19,20]. Initially, the climatological record of cirrus cloud relied on observations as part of weather records before satellites were developed to detect high altitude ice clouds on a global scale [21]. Targeted science projects with research aircraft together with the deployment of ground-based remote sensing technology. Sassen and Mace have provided detailed information about key cloud parameters including ice water content (IWC), ice number concentration (N_{ice}) and ice supersaturation (RH_{ice}) [22]. Many of these projects are described in [19,20,23].

Depending on the measurement approach, the accurate quantification of cirrus properties is subject to a number of limitations. Ground-based observations are limited in their distribution and can be obscured by low clouds. Targeted research flights, despite having sophisticated instrumentation, are limited in their spatial extent. The biggest spatial coverage of cirrus measurements is via spaceborne remote sensing techniques. However, despite the large amount of remote sensing data collected from space, it should be cautioned that there are still many challenges with this approach [23]. In situ measurements on a relevant scale are needed to characterise cirrus properties and to validate the co-existing measurement techniques. The approach described here sits between existing measurement techniques, providing the large spatial coverage of in situ measurements that are not provided by targeted research flights and measuring the size and number density range of cirrus particles that is problematic for satellite remote sensing techniques.

We present the largest in situ cirrus dataset collected to date, both in terms of the quantity and global coverage of data. We present a global analysis of 79 months of in situ cloud measurements from the IAGOS fleet of commercial Airbus aircraft and then focus on identifiable seasonal trends in different regions. The focus of this study is on the Upper Troposphere Lower Stratosphere (UTLS) region split into box domains covering the North Atlantic ($45\text{--}60^\circ \text{ N}$, $11\text{--}5^\circ \text{ W}$), Continental Europe ($43\text{--}53^\circ \text{ N}$, $22^\circ \text{ E--}1^\circ \text{ W}$), the Sub-Tropical Atlantic ($44\text{--}28^\circ \text{ N}$, $11\text{--}53^\circ \text{ W}$), the Tropical Atlantic ($2^\circ \text{ S--}13^\circ \text{ N}$, $18\text{--}43^\circ \text{ W}$), North America ($36\text{--}60^\circ \text{ N}$, $71\text{--}89^\circ \text{ W}$) and South East Asia ($5\text{--}20^\circ \text{ N}$, $120\text{--}100^\circ \text{ E}$).

The aim of this paper was to examine whether the increasingly expansive dataset was representative in a climatological context. We found common identifiable trends in our data, particularly the Northern Hemisphere winter jet stream and the relatively higher cloud fractions in tropical areas attributable to cirrus from thunderstorm outflow. While

targeted research flights provide very detailed in situ measurements of cirrus properties and satellite remote sensing activity gathers data on a global scale, IAGOS and the utilisation of commercial aircraft provides unique opportunities to fill the gap and provide in situ measurements over large areas of the globe and provide the aviation industry with important information about the types of conditions aircraft are exposed to during routine flight.

2. Measurements

Measurements of cloud microphysical properties were made as part of the IAGOS-CORE package of instrumentation on Airbus A330 and A340 aircraft. We analysed an 8-year dataset from the ongoing IAGOS project that was collected by a fleet of 10 aircraft and six international airlines (Air France, Cathay Pacific, China Airlines, Hawaiian Airlines, Iberia and Lufthansa). Measurements of the concentration of cloud particles with equivalent optical diameter (EOD) between 5 and 75 μm were made with a backscatter cloud probe (BCP) mounted on the aircraft fuselage. The instrument (Figure 1a,b) uses a linearly polarized laser (wavelength 658 nm) to detect the backscatter signal from particles that transit through the sample volume. The intensity of this signal is related to the particle size and is used to calculate the concentration of particles detected in flight. Extensive details about the instrument, its calibration and comparison with other instruments and the uncertainties associated with derived particle properties can be found in the technical paper by [24].



Figure 1. (a) Instrument installation on the In-Service Aircraft for a Global Observing System (IAGOS) instrumented Airbus and (b) the backscatter cloud probe (BCP).

A limitation of the measurements compared to those used on research aircraft, however, is the lack of the identification of concentration artefacts due to ice crystal shattering possibly generated by upstream superstructures [25]. To this end, concentration trends are compared as far as possible with near concurrent geo-located measurements from research aircraft, and potential outliers removed from the analyses. We examined clouds measured during the cruise altitude of the aircraft (≥ 10 km).

While we selected the light data above the 10 km altitude level, so the operational ceiling of commercial aircraft means our measurements are limited to an altitude range between 10 km and approximately 12.5 km. In some regions, such as the tropics, cirrus clouds are present at altitudes exceeding this altitude (up to ~ 17 km). The capability of the BCP instrument also means larger ice particles in aged cirrus clouds are potentially missed, while very thin cirrus containing a few small ice particles might also not be detected.

2.1. Global Measurement Distribution

Figure 2 shows the global distribution of BCP measurements (one degree resolution) at high altitude (≥ 10 km) over 79 months between December 2012 and July 2018. This shows that the measurements are extensive across the globe from 43° S to 77° N, with the greatest frequency of measurements focused on commercial air routes over Europe, Africa,

across the Atlantic to North and South America, with another focus of activity on South East Asia. The total hours of flight are shown in Figure 3 with favoured routes having 10 s or even 100 s of hours of measurement points. In total, this measurement approach has provided over 60,000 h of measurement data.

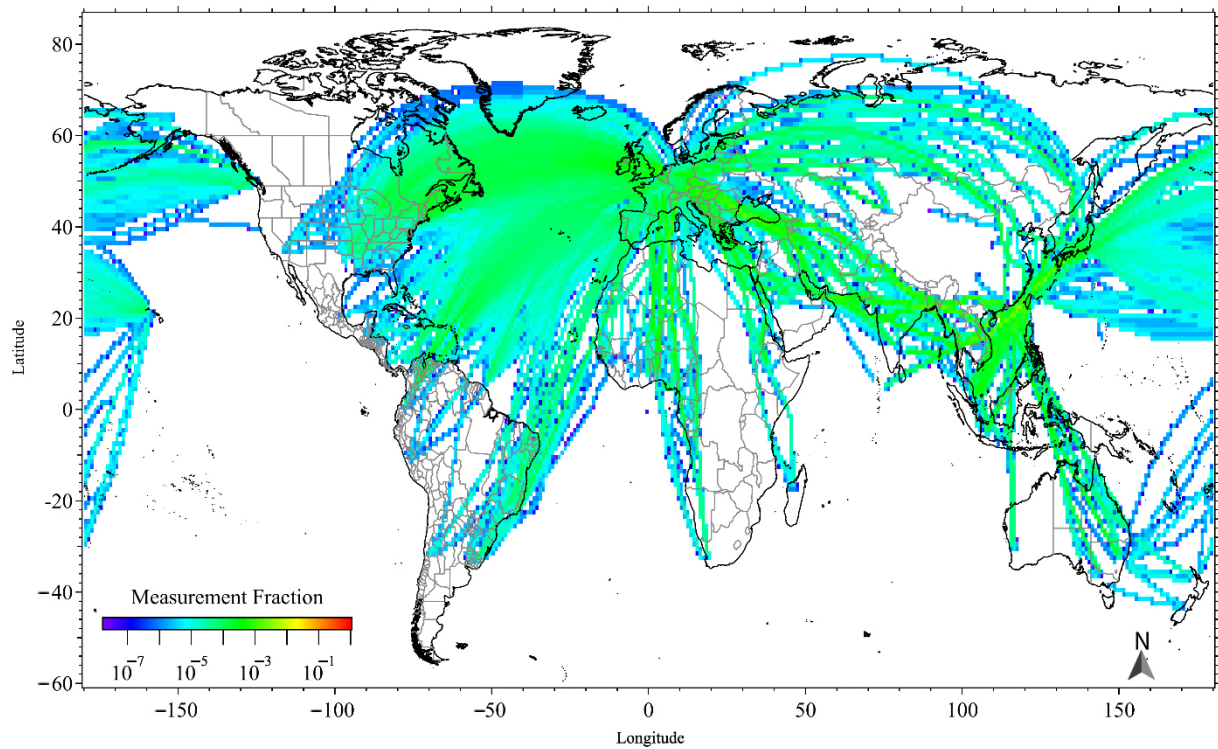


Figure 2. Global measurement fraction from the backscatter cloud probe on the IAGOS fleet of Airbus aircraft.

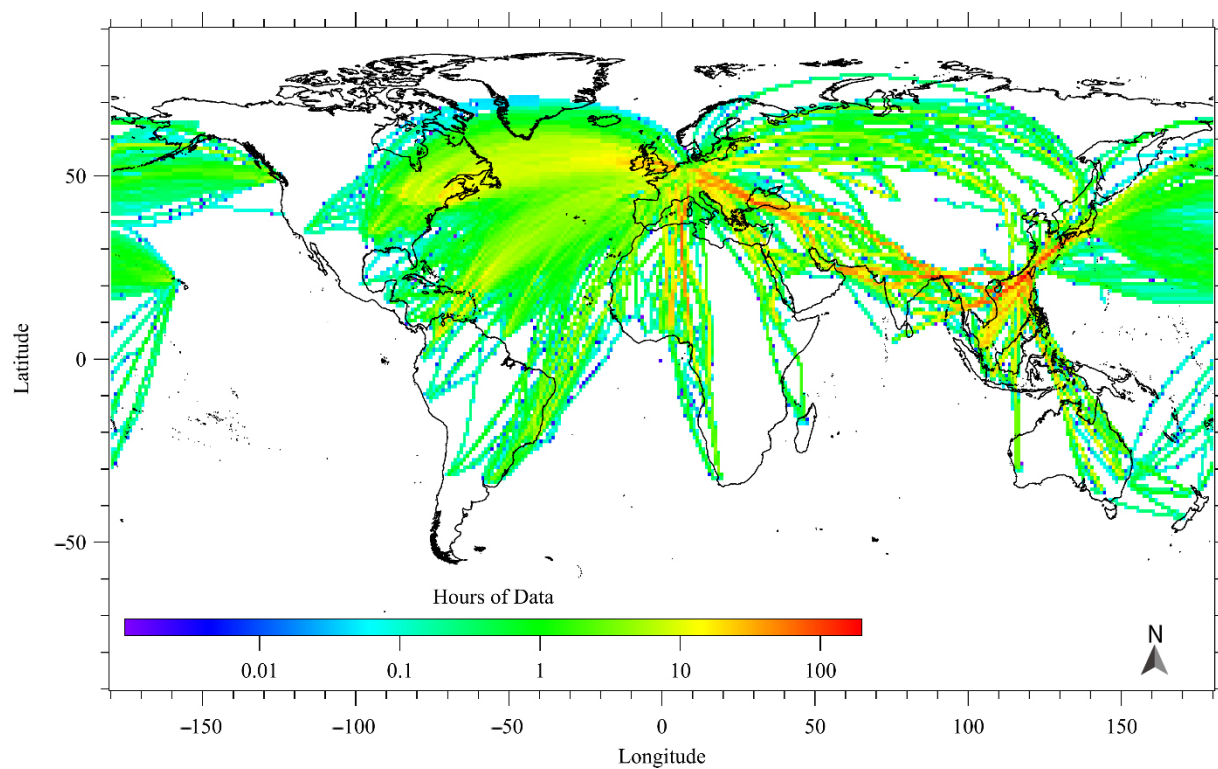


Figure 3. Global measurement hours by the backscatter cloud probe on the IAGOS fleet of Airbus aircraft.

2.2. Cloud Fractions

Figure 4 shows the global cloud fraction of clouds ≥ 10 km sampled by the BCP binned by latitude and longitude (one degree bin resolution). It shows clear regional differences in cloud fraction with higher cloud fractions in regions such as the Inter Tropical Convergence Zone (ITCZ) over the South Atlantic and in South East Asia. In contrast, flight paths over the North Atlantic have much lower cloud fractions. The grey colour in Figure 1b represents a zero cloud fraction that is produced when the BCP has measured no concentrations of cloud particles $\geq 0.05 \text{ cm}^{-3}$.

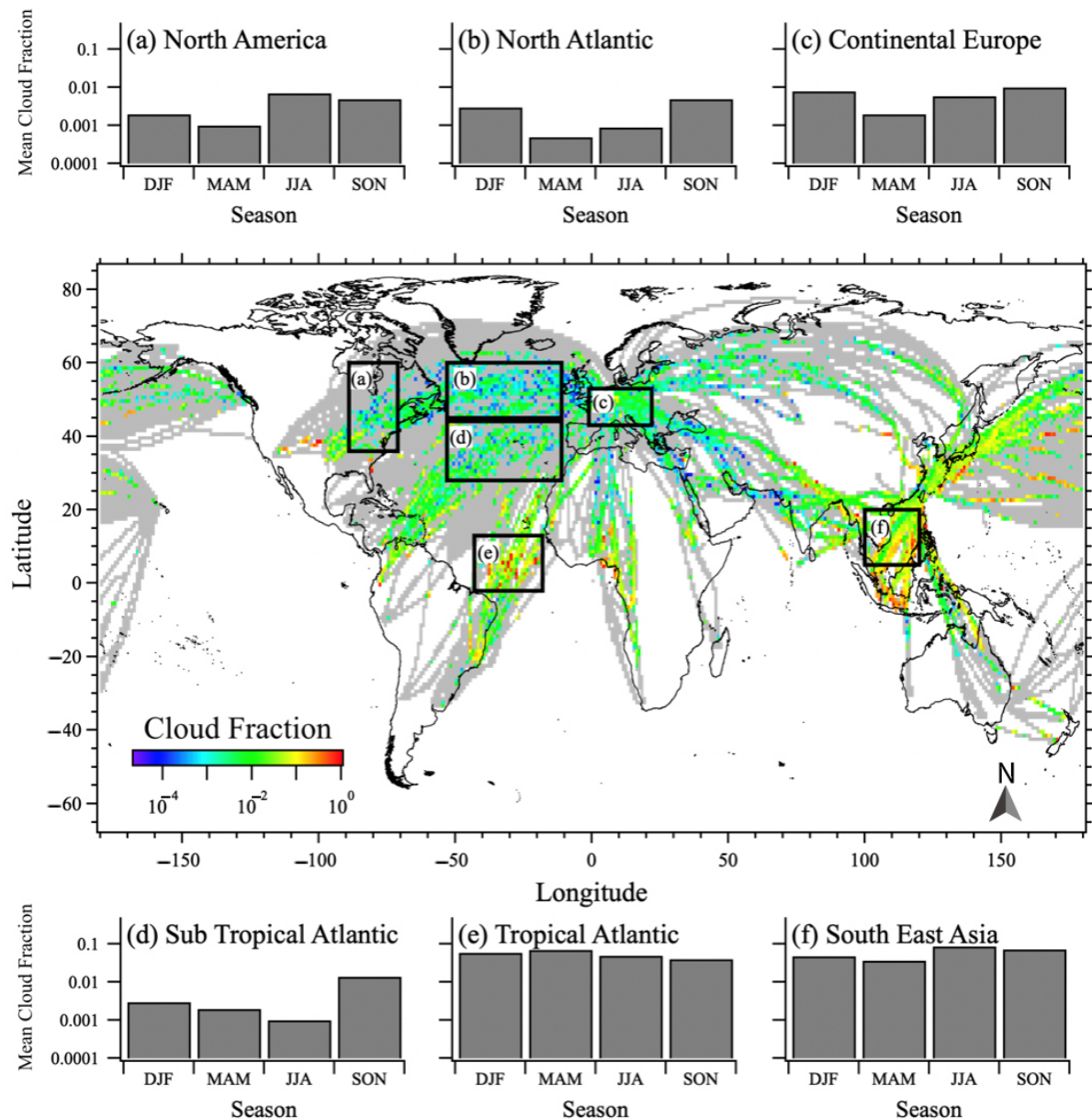


Figure 4. Global cirrus cloud fraction and seasonal mean cirrus cloud fractions for 6 regions. (a) North American; (b) North Atlantic; (c) Continental Europe; (d) Sub Tropical Atlantic; (e) Tropical Atlantic; (f) South East Asia.

The cloud fraction was calculated by taking each 4 second measurement report from the BCP and flagging cloud as present when the reported concentration was $\geq 0.05 \text{ cm}^{-3}$. This low concentration threshold represents 12 detection events and a 30% sampling error. (sampling data points were considered cloud free when this threshold was not met). The

cloud fraction was then calculated as the number of in-cloud points/the number of points in each bin.

The cloud fractions derived here fall between 0.001 and 0.1. These values are lower than others reported from previous retrievals reported in the literature. Chepfer et al. [26] used two different approaches to identify the cloud fractions from spaceborne measurements over a 1-year period between September 2006 and August 2007. They found high cloud fractions of between 0.31 and 0.4 globally. Stubenrauch et al. [27] analysed a range of cloud fraction retrievals (see Figure 1), finding high cloud fractions globally that ranged from about 0.1 to 0.6. Petzold et al., [9] first presented cloud fraction values from the IAGOS dataset for cirrus clouds reporting a range between 0.01 and 0.32. Despite the large range of values described by the different approaches, our dataset generally falls outside this range. Some of the reasons for this discrepancy are described below.

The approach of using a commercial aircraft has produced a dataset that provides information about cloud presence at a single altitude level in the atmosphere which is determined by the altitude of the aircraft. High cloud layers could be present at the same position of the aircraft but at a different altitude level, which would lead to a zero cloud fraction being registered. Other techniques such as spaceborne remote sensing detect high clouds over the full depth of the atmosphere, leading to a much greater chance of cloud detection. Key to Petzold et al., [9] was the selection of data below the thermal tropopause and the exclusion of stratospheric data. In this study, we decided to include all the data available to determine the cloud fractions to provide insight for the aviation industry into conditions of aircraft experience during routine commercial flight. The decision to include generally cloud-free stratospheric data will drastically reduce our cloud fraction values relative to previous studies.

2.3. Seasonal Trends in Cloud Fractions

Based on information about seasonality in different areas of the globe, we selected the six regions identified in the map shown in Figure 4 for further analysis. The Oceanic regions of the North and Sub-Tropical Atlantic were selected to look at the seasonal changes in cloud fraction that are driven by the jet stream storm belts in the mid-latitudes [28]. The North Atlantic high cloud amount is strongly influenced by these seasonal changes, the Sub-Tropical Atlantic was selected for a contrast to the oceanic regions further towards the poles to investigate high cloud changes with increasing distance towards the equator.

The ITCZ marks the “meteorological equator” where surface trade winds converge to produce a zone of increased mean convection, cloudiness and precipitation [29]. The line of convection shifts with the seasons, moving northwards during the Northern Hemisphere spring and summer, and southwards during the Southern Hemisphere spring and summer. The large convective systems produce broad areas of cirrus from convective outflow and we selected two regions to examine this band of activity; the Tropical Atlantic and South East Asia.

The remaining regions, Europe and North America, were chosen for their continental influence and mid-latitude position. This allowed us to look at the relative contributions from the Northern Hemisphere autumn and winter time jet stream together with high clouds produced by convective outflow during the summer months.

Seasonal Variations in Cloud Fraction by Region

Here, we present 6 regions and calculate the cloud fraction by season. These regions are described and highlighted in Figure 4. The seasons are split into December, January, February (DJF), March, April May (MAM), June, July August (JJA) and September, October, November (SON). The global map shows the one degree binned annual cloud fraction value, the grey colours represent areas in which measurements were made but no cloud was observed. The black boxes enclose the domains that were selected for further analysis by season. The bar charts surrounding the global map represent cloud fraction split by season for each region.

High cloud fraction over continental Europe was found to be strongly seasonal (Figure 4a). During the Northern Hemisphere autumn (SON) and winter months (DJF), cloud fractions showed the strongest signal with the domain mean cloud fractions of 0.01 and 0.008 for SON and DJF, respectively. After the winter cloud fraction drops significantly during MAM before rising again in the JJA period to 0.006.

Over the North Atlantic, the cloud fraction (Figure 4d) exhibits a maximum occurrence during the SON and DJF periods. The peak cloud fraction value is during SON with a value of 0.005. The lowest cloud fraction is observed in MAM.

The Sub-Tropical Atlantic (Figure 4e) also had a peak cloud fraction (0.014) during SON. During the remaining periods, DJF, MAM and JJA cloud fractions were <0.004 with the minimum value recorded during the JJA period (0.001).

North America peak cloud fractions (Figure 4c) occur in the summer (JJA) with values of 0.007. There is also increased cloud fractions during the autumn (SON). The lowest fractions are seen during MAM.

Variations in South East Asia (Figure 4b) are less pronounced but have a peak during the JJA and SON periods of 0.09 and 0.07, respectively. The lowest cloud fractions are observed during MAM.

The Tropical Atlantic region is dominated by the convective activity produced by the ITCZ. In comparison with regions of the globe further towards the poles, the cloud fractions are higher in all seasons (Figure 4f). However, our data still exhibit variations throughout the four seasons, with MAM showing the greatest cloud fraction values. The lowest cloud fractions were observed during SON.

3. Discussion

Contributions to the understanding of global cirrus cloud properties has evolved over time from observational reporting at the surface to remote sensing from both space borne and ground based instrumentation designed to study the key microphysical and macrophysical properties of cirrus clouds. In addition to remote sensing techniques, relatively small scale but highly targeted in situ measurements have vastly improved our understanding of the small scale processes governing cirrus cloud formation, evolution and radiative properties [19]. Whilst these targeted airborne research campaigns cover a range of different meteorological conditions, these may not necessarily provide a statistically representative distribution of cirrus cloud frequencies and properties in the UTLS region. To address this in the long term, global satellite remote sensing is the ideal approach, however, retrievals of cirrus microphysical properties can have limitations such as altitude resolution and the calculation of number concentrations, which remain a challenge [13]. IAGOS is an opportunity to add to the global cirrus climatology, and here we describe some of the initial results from this global in situ dataset.

A key feature of the mid latitudes in the Northern Hemisphere was the signature of maximum cloud fractions in the autumn (SON) and winter (DJF) months. The maritime North Atlantic (Figure 4b) showed this variation the most strongly, with significant increases in these periods and much lower cloud fractions in the spring and summer. The driving force for these changes is the strengthening of the polar vortex during the Northern Hemisphere winter and the storm tracks that this produces across the North Atlantic. This variation was also evident over continental Europe (Figure 4c). In addition to this, there was also increased cloud fractions during the summer period (JJA), presumably due to convective activity over the land producing cirrus outflow from thunderstorm outflow.

The North American region (Figure 4a), although showing the signature of the jet stream-driven cirrus in the winter months, was dominated by higher cloud fractions during the summer, likely to be a result of the strong thunderstorm systems that develop over the United States of America (USA) during this season and the associated convective cirrus outflow. The Sub-Tropical Atlantic (Figure 4d) had a jet stream cirrus signature during autumn, but the trend overall was less evident than for the North Atlantic region, which is

expected as the distance from the polar front increases and the impact from mid-latitude depressions decreases.

The tropical regions of the Atlantic and South East Asia both exhibited relatively high cloud fractions when compared to the mid-latitude continents and oceanic regions. The outflow cirrus in these regions is very dominant, coinciding with the monsoon season in South East Asia but evident the whole year. Over the Tropical Atlantic, the outflow cirrus is most likely to be associated with the ITCZ.

The cloud fractions presented for each region were the result of an approach that averages the data from each of the seasons between December 2011 and July 2018. When we examined individual years, we found significant inter-annual variability in the cloud fractions. While caution should be taken about the measurement bias (data collection focused on busy air corridors) the variability in some regions may represent large scale cyclical climate phenomenon. One example is the El Niño Southern Oscillation (ENSO), a key driver of weather patterns over the Tropical Pacific Ocean region. Although the annual cycle is most dominant at all longitudes and latitudes, Eleftheratos et al., found that ENSO has a strong influence on high cloud fraction in the Western Pacific, with 6.2% of the variance explained by ENSO [30]. The contribution to variability by other known cycles that influence weather patterns, such as the QBO, 11-year-solar cycle and long-term-trend-related cloud components was estimated to about 1.0, 0.1 and 0.3%, respectively.

The South East Asia region exhibited a significant increase in cirrus cloud fraction during 2016 centred around the JJA and SON period (Figure 5). Although our measurement period is limited in the context of the ENSO signal, this is consistent with the findings reported by Virts and Wallace that found a shift in peak cloudiness towards the maritime continent during La Nina [31].

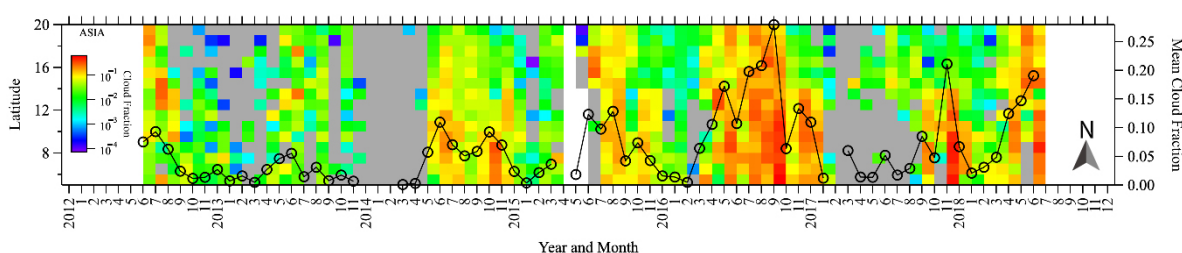


Figure 5. Hövmoller diagram during the period 2012–2018 for the Asian region showing monthly latitudinal averaged cirrus cloud fraction and the monthly averaged cirrus cloud fraction for the entire region.

In the mid-latitude regions we studied, cloud fractions are also dominated by the seasonal cycle, while large scale dynamics, such as the North Atlantic Oscillation, also contribute to the inter-annual variability. Eleftheratos et al., found a small positive correlation between cloud cover in the North Atlantic Flight Corridor (NAFC) of 0.3. They also found trends in cloud cover of +1.6% per decade, demonstrating the importance of the continued long-term monitoring of this region [32].

4. Conclusions

To conclude, we presented a global dataset of cloud particle number collected as part of IAGOS. We report a number of key findings:

- We examined regions of the globe covering oceanic, continental and tropical areas to see how representative the dataset was in demonstrating common seasonal trends in each region.
- We found that the measurements were able to demonstrate seasonal changes in the cloud fraction associated with the Northern Hemisphere mid-latitude jet stream and the relatively higher cloud fractions found in tropical regions as a result of thunderstorm cirrus outflow.
- This dataset and the ongoing measurements as part of IAGOS are an important addition to the already existing infrastructure for the monitoring of high-altitude

clouds that include remote sensing (ground based and space borne) and targeted research flights.

- The measurements also provide an excellent tool for the aviation industry to investigate the influence of adverse conditions on aircraft performance.
- Cloud fraction calculations included both tropospheric and stratospheric data to assess the conditions in the context of commercial flight paths. Further works are needed to compare the cloud fraction values presented in this paper with previous research.

Author Contributions: Conceptualization, G.L., M.G. and T.C.; formal analysis, G.L.; resources, T.C., M.G., D.B., M.K. and P.A.; writing—original draft preparation, G.L.; writing—review and editing, G.L., T.C., M.G., P.A., D.B. and M.K.; All authors have read and agreed to the published version of the manuscript.

Funding: This work was funded by the National Centre for Atmospheric Science (NCAS) and the University of Manchester. This work is part of In-Service Aircraft for a Global Observing System (IAGOS) (www.iagos.org).

Conflicts of Interest: The authors declare no conflict of interest.

References

- Petzold, A.; Thouret, V.; Gerbig, C.; Zahn, A.; Brenninkmeijer, C.A.M.; Gallagher, M.; Hermann, M.; Pontaud, M.; Ziereis, H.; Boulanger, D.; et al. Global-scale atmosphere monitoring by in-service aircraft—Current achievements and future prospects of the European Research Infrastructure IAGOS. *Tellus B Chem. Phys. Meteorol.* **2015**, *67*, 1–24. [[CrossRef](#)]
- Bojinski, S.; Verstraete, M.; Peterson, T.C.; Richter, C.; Simmons, A.; Zemp, M. The Concept of Essential Climate Variables in Support of Climate Research, Applications, and Policy. *Bull. Am. Meteorol. Soc.* **2014**, *95*, 1431–1443. [[CrossRef](#)]
- Berkes, F.; Neis, P.; Schultz, M.; Bundke, U.; Rohs, S.; Smit, H.G.J.; Wahner, A.; Konopka, P.; Boulanger, D.; Nédélec, P.; et al. In situ temperature measurements in the upper troposphere and lowermost stratosphere from 2 decades of IAGOS long-term routine observation. *Atmos. Chem. Phys. Discuss.* **2017**, *17*, 12495–12508. [[CrossRef](#)]
- Filges, A.; Gerbig, C.; Chen, H.; Franke, H.; Klaus, C.; Jordan, A. The IAGOS-core greenhouse gas package: A measurement system for continuous airborne observations of CO₂, CH₄, H₂O and CO. *Tellus B Chem. Phys. Meteorol.* **2015**, *67*, 27989. [[CrossRef](#)]
- Filges, A.; Gerbig, C.; Rella, C.W.; Hoffnagle, J.; Smit, H.; Krämer, M.; Spelten, N.; Rolf, C.; Bozóki, Z.; Buchholz, B.; et al. Evaluation of the IAGOS-Core GHG package H₂O measurements during the DENCHAR airborne inter-comparison campaign in 2011. *Atmos. Meas. Tech.* **2018**, *11*, 5279–5297. [[CrossRef](#)]
- Clark, H.; Sauvage, B.; Thouret, V.; Nédélec, P.; Blot, R.; Wang, K.; Smit, H.; Neis, P.; Petzold, A.; Athier, G. The first regular measurements of ozone, carbon monoxide and water vapour in the Pacific UTLS by IAGOS the first regular measurements of ozone, carbon monoxide and water vapour in the Pacific UTLS by IAGOS. *Tellus B Chem. Phys. Meteorol.* **2015**, *67*, 28385. [[CrossRef](#)]
- Cohen, Y.; Petetin, H.; Thouret, V.; Marécal, V.; Josse, B.; Clark, H.; Sauvage, B.; Fontaine, A.; Athier, G.; Blot, R.; et al. Climatology and long-term evolution of ozone and carbon monoxide in the upper troposphere–lower stratosphere (UTLS) at northern midlatitudes, as seen by IAGOS from 1995 to 2013. *Atmos. Chem. Phys. Discuss.* **2018**, *18*, 5415–5453. [[CrossRef](#)]
- Gaudel, A.; Cooper, O.R.; Ancellet, G.; Barret, B.; Boynard, A.; Burrows, J.P.; Clerbaux, C.; Coheur, P.-F.; Cuesta, J.; Cuevas, E.; et al. Tropospheric Ozone Assessment Report: Present-day distribution and trends of tropospheric ozone relevant to climate and global atmospheric chemistry model evaluation. *Elem. Sci. Anthr.* **2018**, *6*. [[CrossRef](#)]
- Petzold, A.; Krämer, M.; Neis, P.; Rolf, C.; Rohs, S.; Berkes, F.; Smit, H.G.J.; Gallagher, M.; Beswick, K.; Lloyd, G.; et al. Upper tropospheric water vapour and its interaction with cirrus clouds as seen from IAGOS long-term routine in situ observations. *Faraday Discuss.* **2017**, *200*, 229–249. [[CrossRef](#)]
- Beswick, K.; Baumgardner, D.; Gallagher, M.; Raga, G.B.; Minnis, P.; Spangenberg, D.A.; Volz-Thomas, A.; Nédélec, P.; Wang, K.-Y. Properties of small cirrus ice crystals from commercial aircraft measurements and implications for flight operations. *Tellus B Chem. Phys. Meteorol.* **2015**, *67*, 27876. [[CrossRef](#)]
- Jones, H.M.; Haywood, J.; Marenco, F.; O’Sullivan, D.; Meyer, J.; Thorpe, R.; Gallagher, M.W.; Krämer, M.; Bower, K.N.; Rädcl, G.; et al. A methodology for in-situ and remote sensing of microphysical and radiative properties of contrails as they evolve into cirrus. *Atmos. Chem. Phys. Discuss.* **2012**, *12*, 8157–8175. [[CrossRef](#)]
- Kärcher, B. Formation and radiative forcing of contrail cirrus. *Nat. Commun.* **2018**, *9*, 1–17. [[CrossRef](#)] [[PubMed](#)]
- Burkhardt, U.; Kärcher, B. Process-based simulation of contrail cirrus in a global climate model. *J. Geophys. Res. Space Phys.* **2009**, *114*, 16201. [[CrossRef](#)]
- Minnis, P.; Schumann, U.; Doelling, D.R.; Gierens, K.M.; Fahey, D.W. Global distribution of contrail radiative forcing. *Geophys. Res. Lett.* **1999**, *26*, 1853–1856. [[CrossRef](#)]
- Fahey, D.W.; Schumann, U.; Ackerman, S.; Artaxo, P.; Boucher, O. Aviation-produced aerosol and cloudiness. *Changes* **1999**, *3*, 4.

16. Baran, A.J. From the single-scattering properties of ice crystals to climate prediction: A way forward. *Atmos. Res.* **2012**, *112*, 45–69. [CrossRef]
17. Boucher, O.; Randall, D.; Artaxo, P.; Bretherton, C.; Feingold, G.; Forster, P.; Rasch, P. Clouds and aerosols. In *Climate Change 2013: The Physical Science Basis. Contribution of Working Group I to the Fifth Assessment Report of the Intergovernmental Panel on Climate Change*; Cambridge University Press: Cambridge, UK, 2013; pp. 571–657.
18. Kärcher, B. Cirrus Clouds and Their Response to Anthropogenic Activities. *Curr. Clim. Chang. Rep.* **2017**, *3*, 45–57. [CrossRef]
19. Krämer, M.; Rolf, C.; Luebke, A.; Afchine, A.; Spelten, N.; Costa, A.; Meyer, J.; Zöger, M.; Smith, J.; Herman, R.L.; et al. A microphysics guide to cirrus clouds—Part 1: Cirrus types. *Atmos. Chem. Phys. Discuss.* **2016**, *16*, 3463–3483. [CrossRef]
20. Krämer, M.; Rolf, C.; Spelten, N.; Afchine, A.; Fahey, D.; Jensen, E.; Khaykin, S.; Kuhn, T.; Lawson, P.; Lykov, A.; et al. A Microphysics Guide to Cirrus—Part II: Climatologies of Clouds and Humidity from Observations. *Atmos. Chem. Phys. Discuss.* **2020**, *20*, 12569–12608. [CrossRef]
21. Sassen, K.; Wang, Z.; Liu, D. Global distribution of cirrus clouds from CloudSat/Cloud-Aerosol Lidar and Infrared Pathfinder Satellite Observations (CALIPSO) measurements. *J. Geophys. Res. Space Phys.* **2008**, *113*, 1–12. [CrossRef]
22. Sassen, K.; Mace, G. *Ground-Based Remote Sensing of Cirrus Clouds*; Oxford: New York, NY, USA, 2002; pp. 168–209.
23. Lawson, R.P.; Woods, S.; Jensen, E.J.; Erfani, E.; Gurganus, C.; Gallagher, M.; Connolly, P.J.; Whiteway, J.; Baran, A.J.; May, P.; et al. A Review of Ice Particle Shapes in Cirrus formed In Situ and in Anvils. *J. Geophys. Res. Atmos.* **2019**, *124*, 10049–10090. [CrossRef]
24. Beswick, K.M.; Baumgardner, D.; Gallagher, M.; Volz-Thomas, A.; Nedelec, P.; Wang, K.-Y.; Lance, S. The backscatter cloud probe—A compact low-profile autonomous optical spectrometer. *Atmos. Meas. Tech.* **2014**, *7*, 1443–1457. [CrossRef]
25. Korolev, A.; Field, P.R. Assessment of the performance of the inter-arrival time algorithm to identify ice shattering artifacts in cloud particle probe measurements. *Atmos. Meas. Tech.* **2015**, *8*, 761–777. [CrossRef]
26. Chepfer, H.; Cesana, G.; Winker, D.; Getzewich, B.; Vaughan, M.; Liu, Z. Comparison of two different cloud climatologies derived from CALIOP-attenuated backscattered measurements (level 1): The CALIPSO-ST and the CALIPSO-GOCCP. *J. Atmos. Ocean. Technol.* **2013**, *30*, 725–744. [CrossRef]
27. Stubenrauch, C.J.; Rossow, W.B.; Kinne, S.; Ackerman, S.; Cesana, G.; Chepfer, H.; Maddux, B.C. Assessment of global cloud datasets from satellites: Project and database initiated by the GEWEX radiation panel. *Bull. Am. Meteorol. Soc.* **2013**, *94*, 1031–1049. [CrossRef]
28. Wylie, D.P.; Menzel, W.P.; Woolf, H.M.; Strabala, K.I. Four Years of Global Cirrus Cloud Statistics Using HIRS. *J. Clim.* **1994**, *7*, 1972–1986. [CrossRef]
29. Waliser, D.; Jiang, X. Tropical Meteorology and Climate | Intertropical Convergence Zone. Available online: http://climvar.org/jiang/pub/Duane_ATM2_00417.pdf (accessed on 30 December 2020).
30. Eleftheratos, K.; Zerefos, C.S.; Varotsos, C.; Kapsomenakis, I. Interannual variability of cirrus clouds in the tropics in El Niño Southern Oscillation (ENSO) regions based on International Satellite Cloud Climatology Project (ISCCP) satellite data. *Int. J. Remote Sens.* **2011**, *32*, 6395–6405. [CrossRef]
31. Virts, K.S.; Wallace, J.M. Annual, Interannual, and Intraseasonal Variability of Tropical Tropopause Transition Layer Cirrus. *J. Atmos. Sci.* **2010**, *67*, 3097–3112. [CrossRef]
32. Eleftheratos, K.; Zerefos, C.S.; Zanis, P.; Balis, D.S.; Tselioudis, G.; Gierens, K.; Sausen, R. A study on natural and manmade global interannual fluctuations of cirrus cloud cover for the period 1984–2004. *Atmos. Chem. Phys. Discuss.* **2007**, *7*, 2631–2642. [CrossRef]